



# Mechanical and damping properties of resin transfer moulded jute-carbon hybrid composites

Sam Ashworth, Jem Rongong, Peter Wilson, James Meredith\*

Department of Mechanical Engineering, University of Sheffield, Sir Frederick Mappin Building, Mappin Street, Sheffield, S1 3JD, UK

## ARTICLE INFO

### Article history:

Received 18 May 2016

Received in revised form

15 July 2016

Accepted 17 August 2016

Available online 20 August 2016

### Keywords:

Hybrid

Internal friction/damping

Mechanical testing

Resin transfer moulding

## ABSTRACT

Hybrid composites with carbon and natural fibres offer high modulus and strength combined with low cost and the ability to damp vibration. This study investigates carbon (CFRP), jute (NFRP) and hybrid (HFRP) fibre reinforced polymers manufactured using the resin transfer moulding process.

Tensile strength reduced with increasing injection pressure for NFRP (72.7 MPa at 4 bar, 45.5 MPa at 8 bar) and HFRP (98.4 MPa at 4 bar, 92.4 MPa at 8 bar). The tensile modulus for HFRP (15.1 GPa) was almost double that for NFRP (8.2 GPa) and one third of CFRP (44.2 GPa).

Loss factor reduced at small strains ( $10^{-4}$ ) with increasing pressure for NFRP (0.0123 at 4 bar, 0.0112 at 8 bar) and HFRP (0.0048 at 4 bar, 0.0038 at 8 bar) but all were greater than CFRP (0.0024).

Increased injection pressure improved the surface properties and prevented read through of the weave pattern, NFRP ( $R_a = 2.15 \mu\text{m}$  at 4 bar,  $1.51 \mu\text{m}$  at 8 bar) and HFRP ( $R_a = 1.80 \mu\text{m}$  at 4 bar,  $1.42 \mu\text{m}$  at 8 bar). Hybridisation of low cost, sustainable jute with carbon fibre offers a more sustainable and economic alternative to CFRPs with excellent damping properties.

© 2016 The Authors. Published by Elsevier Ltd. This is an open access article under the CC BY license (<http://creativecommons.org/licenses/by/4.0/>).

## 1. Introduction

Fibre reinforced polymer composites are now applied widely in industry where it is desirable to reduce mass by taking advantage of their high specific strength and stiffness. Carbon fibres are energy intensive to manufacture making them expensive financially and environmentally [1]. An alternative approach is to use natural fibres which are renewable, have low embodied energy, low cost and low density [2]. However, they have poor mechanical properties, high variation, sensitivity to moisture and poor adhesion between fibre and matrix [3]. Recycling of carbon fibre reinforced polymers (CFRPs) at their end of life is the subject of intense research focused on extracting value from both fibres and matrix [4–7]. Natural fibre reinforced polymers (NFRPs) are either composted or burnt for energy recovery at their end of life with the primary advantage of being carbon neutral [8].

Hybrid fibre reinforced polymers (HFRPs) use two or more reinforcements with a single matrix giving rise to a more favourable balance between advantages and disadvantages of the core components [9,10]. The combination of a high strength fibre such as

glass or carbon with natural fibres can lead to a desirable mix of performance, cost and environmental attributes. Glass fibre epoxy composites have been hybridised with jute [11], kenaf [12], sisal [13] and bamboo [14]. Carbon-flax HFRPs have demonstrated enhanced mechanical properties versus NFRPs and improved damping [15,16].

NFRPs rely on mechanical interaction between fibre and matrix versus chemical bonding with synthetic fibres making them better able to damp vibrations [17]. Damping in NFRPs is via the properties of plant fibres including entanglement, voids in the lumen, heterogeneity of the cell wall and reversible hydrogen bonding in the cell wall [18–20]. Damping in NFRPs can also be tailored by using fibre twist and crimp [21].

CFRPs have poor damping characteristics and are highly resonant [22]. This is beneficial for applications such as musical instruments, however when applied in structures subject to vibration the lack of damping can cause resonant vibration. CFRPs have high specific stiffness and low levels of damping with loss factors typically below 0.002 compared with NFRPs with loss factors of 0.01 or higher [22]. A heavy structure with high inherent damping (i.e. high capacity for dissipate vibration energy) is less likely to suffer from vibration problems.

Resin transfer moulding (RTM) is popular in the automotive and aerospace industries since it is a clean and eco-friendly closed

\* Corresponding author.

E-mail address: [j.meredith@sheffield.ac.uk](mailto:j.meredith@sheffield.ac.uk) (J. Meredith).

mould process. RTM requires placement of a fibre preform into a closed mould followed by injection of liquid resin under pressure to infiltrate and wet the fibres and prevent void formation [23]. It is a process able to deliver high quality components at the required volume and cost to make them practical for aerospace and when used with high pressure for a short cycle time, the automotive industry [24]. Studies have shown that it can improve inter laminar shear strength, save weight, reduce manufacturing time, improve surface finish and reduce cost [25].

Process parameters influence the way a composite is formed during moulding through events such as air entrapment and wetting which can lead to excessive voidage, also known as porosity within the composite [26]. The tensile properties, flexural strength, fatigue resistance, susceptibility to weathering and consistency of strength are all affected by an increase in void content [27]. Irrespective of the type of matrix, the type of dry fibre, or the moulding process used, the interlaminar shear strength of the composite decreases by approximately 7% for every 1% increase in void content although this does not apply to 3D woven or discontinuous fibre composites [26]. Process parameters including resin injection rate, resin injection pressure and temperature are widely known to affect void formation. Understanding how each parameter affects void formation is critical in the design of an optimum resin transfer moulding process [28].

This study focuses on a family of natural fibres known as ‘bast’ fibres; they are collected from the skin or inner bark on the stem of certain plants, mainly dicotyledonous. The specific type of fibre being investigated is jute. In terms of usage, production and global consumption it is second only to cotton, it is significantly less energy intensive to manufacture than carbon fibre and low cost at less than £500 per tonne compared with £770–7500 per tonne for carbon [29,30]. This work examines the performance of natural, hybrid and carbon epoxy composites manufactured via RTM at two different pressures. Property evaluation includes the sensitivity of the flexural modulus and loss factor to the dynamic strain, behaviour which has not been reported elsewhere for natural and hybrid composites.

## 2. Experimental procedure

### 2.1. Materials

A 199 gsm 2 × 2 twill 3K-T300 carbon fibre fabric (Sigmatec, UK) and a 550 gsm 2 × 2 twill jute fabric (Biotex, UK) were used throughout this work. The fabrics were cut into 28 cm × 28 cm plies before being inserted into the mould cavity with all plies laid at 0°. A low viscosity epoxy resin suitable for RTM was used, DR2188 (Delta Resins, UK) with hardener HY2188 (Delta Resins, UK) and mixed at a ratio of 100 parts by mass of epoxy with 32 parts by mass of hardener.

### 2.2. Manufacture

A steel RTM tool was designed to manufacture a panel 300 × 300 × 3 mm. It had a gating system which utilised convergent flow from all sides and a vacuum port in the centre of the panel (Fig. 1). Resin was injected via a Hypaject (Magnum Venus Products, UK). Before moulding five coats of release agent (227CEE, Marbo-coat, UK) were added to the mould surfaces. An initial study was undertaken to establish the level of fibre compression required to prevent fibre wash and the final layouts for each panel are shown in Table 1. The thickness of the fibre pack was measured using a Vernier calliper. For each material one panel was manufactured at 4 bar and another at 8 bar injection pressure. Fibre volume fraction (FVF) was calculated using the formula below using number of plies

( $n$ ), fabric areal weight ( $A_w$ ), fibre density and laminate thickness ( $d$ ). Fibre density for a T300 fibre is 1.76 g/cm<sup>3</sup> (Torayca) and 1.46 g/cm<sup>3</sup> for jute [31].

$$V_f = \frac{nA_w}{\rho_f d}$$

Once mixed the resin was drawn into the injector under vacuum and left to degas for 5 min. The mould was then evacuated and the resin injected into the RTM tool at a constant pressure as set on the Hyperject. After 5–10 min the resin had passed through the fibre stack and was visible in the vacuum line. The vacuum line was then clamped off and pressure on the resin feed maintained for 1 min before also being clamped off. The resin filled mould was then left to cure for 12 h at room temperature. In this work the resin and RTM variables were set to deliver a quality panel rather than a fast process. After cure the panel was ejected and post cured with the following cycle: 40 °C for 2 h, 60 °C for 2 h, 80 °C for 2 h, 100 °C for 2 h and 120 °C for 12 h and then cooled slowly to room temperature. All ramp rates were set to 2 °C per minute.

## 3. Analysis

### 3.1. Dimensional study

Each panel was cut along its centre line and its thickness measured at 10 evenly spaced points using a Vernier calliper.

### 3.2. Tensile testing

Ultimate tensile strength and tensile modulus were determined according to the American Society for Testing and Materials (ASTM) D3039/DB3039M. A minimum of five samples were cut from each panel with dimensions 250 × 25 mm. Glass fibre reinforced end tabs were bonded onto each sample with epoxy resin (Araldite Rapid, Huntsman Advanced Materials, UK) leaving a gauge length of 150 mm. Tests were carried out on a Mayes DH50 servo hydraulic test machine with a calibrated 100 kN load cell. Tensile modulus was calculated between 0.001 and 0.003 strain according to the standard.

### 3.3. Dynamic testing

The loss factor ( $\eta$ ) and flexural modulus ( $E_f$ ) of the materials were determined from free vibration tests on cantilever beam specimens. Test specimens were cut parallel to the 0° fibre alignment axis with dimensions 250 × 12.5 mm. End tabs, 50 mm in length, were created from E-glass/epoxy composite and bonded to the surface of one end of the specimens using epoxy resin (Araldite Rapid, Huntsman Advanced Materials, UK).

Tests on each specimen involved measurement of the free response following a manual deflection of the tip. The specimen was set up as a cantilever beam by clamping the end tab into a heavy block. After manual deflection of the tip, the response of the beam at a location 58 mm from the clamp, was measured using a 1605-10 laser displacement probe (Micro-Epsilon, UK). To minimise noise in the signal, an opaque sticker was placed on the specimen to prevent the laser beam passing through the material. The response was captured digitally using a sampling rate of 2560 Hz using a SigLab2 data acquisition system. The voltage induced in the laser probe was converted to displacement using a conversion of 10 mm/V stated by the probe manufacturer.

The damping ratio  $\zeta$  and the natural frequency  $\omega_n$  were determined from the free response data using Matlab software. As the damping was assumed to be light, but with some nonlinearity, a

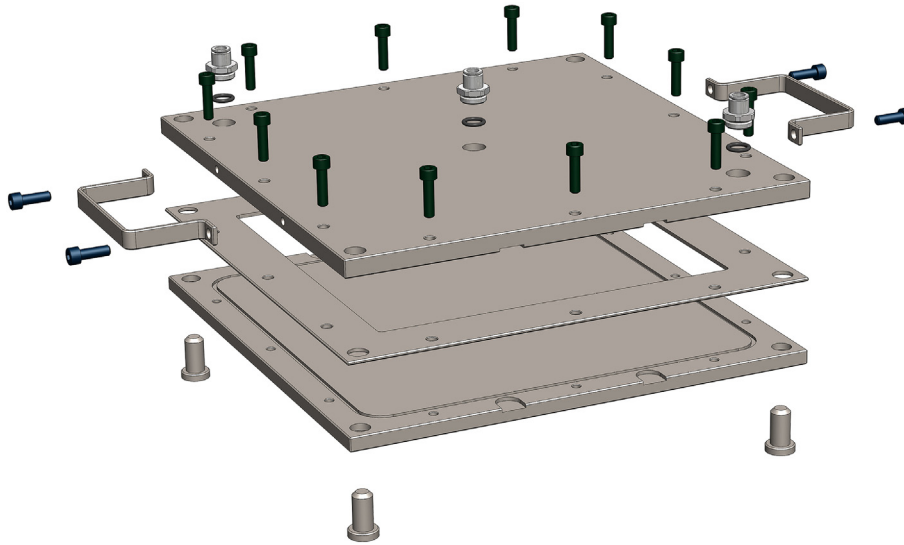


Fig. 1. Exploded view of RTM tool for manufacture of composite panels.

Table 1  
Layup details for each panel type.

Material type	Jute (NFRP)	Hybrid (HFRP)	Carbon (CFRP)
Ply composition	3 plies jute	1 carbon – 3 jute – 1 carbon	14 carbon
Thickness of the dry fibre pack (mm)	4.2	4.7	3.5
Calculated FVF	26.9%	28.9%	45.2%

modification to the standard logarithmic decrement approach was used. The times and amplitudes of the peaks and troughs over the desired part of the response were first identified and the natural frequency obtained from the mean period between individual points. An example is given from the 4 bar NFRP sample in Fig. 2.

If damping is linear viscous, a plot of the logarithm of successive peak (or trough) amplitudes against time yields a straight line. Assuming nonlinearity in damping, low-order polynomials were fitted to the measured data points. This was done separately for peaks and troughs and the average taken to eliminate the effects of static bias caused, for example, by slow realignment of the equilibrium point in viscoelastic specimens. Results of a 3rd order polynomial fit for the 4 bar NFRP sample are shown in Fig. 3.

The instantaneous logarithmic decrement at any time was then

obtained from the gradient of the mean line using:

$$\delta = -\frac{g}{\omega_n}$$

where  $g$  is the gradient of the natural logarithm of amplitude with respect to time and  $\omega_n$  is the natural frequency in Hz. Note that the natural frequency did not change appreciably with amplitude for any of the specimens. The damping ratio  $\zeta$  was then calculated using:

$$\zeta = \frac{1}{\sqrt{1 + \left(\frac{2\pi}{\delta}\right)^2}}$$

As the damping levels were low, the undamped and damped

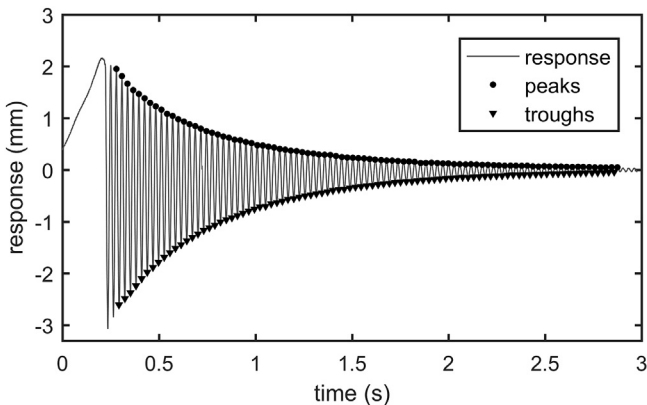


Fig. 2. Free vibration response demonstrating selected peak and trough points for 4 barb NFRP.

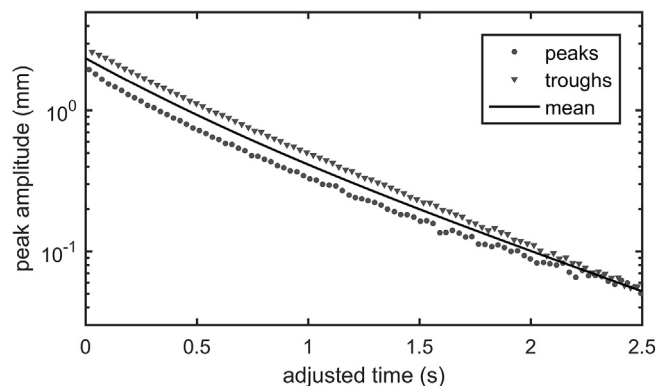


Fig. 3. Polynomial curve fit to test data.

natural frequencies were more or less identical and therefore assumed to be the same. The flexural modulus  $E_f$  was then obtained from:

$$E_f = \frac{48\pi^2 \rho \omega_n^2 L^4}{\beta^4 t^2}$$

where  $\rho$  is the density,  $L$  is the length of the beam outside the clamp,  $t$  is the thickness and  $\beta = 1.875104$  is a constant that accounts for the mode shape. As measurements were taken at the natural frequency, the loss factor  $\eta$  in each case was obtained from:

$$\eta = 2\zeta$$

For each test, the spread of peak and trough data points from the fitted polynomial had a standard deviation of less than 4%. Eight responses were recorded for each material and values of loss factor and flexural modulus were averaged across this range. The tests showed a high level of repeatability with standard deviations for modulus and loss factor being less than 0.5% and 5% respectively. It was considered more useful to relate loss factor to peak strain rather than time or deflection levels as it is more general. The peak strain was estimated assuming the deformation of the composite beam was similar to that of a homogeneous Euler-Bernoulli beam. The result from the 4 bar NFRP sample is provided in Fig. 4 and shows the extent of the scatter from different tests.

### 3.4. Optical microscopy

The corner of each panel was removed with a cut at 45° to the fibre direction. Each sample was mounted in EpoFix (Struers, UK) with EpoDye (Struers, UK), and polished using an Isomet (Buehler, UK) with the following procedure: P1200 abrasive, 9  $\mu\text{m}$  diamond polish, 6  $\mu\text{m}$  diamond polish and 0.05  $\mu\text{m}$  polish. Samples were examined using a Fusion vision system (Qioptiq, UK) with a 5 mega pixel camera (Paxcam, USA). Six images of each sample were taken at 8 $\times$  objective and analysed with Pax-it software (Paxcam, USA) to determine the void content and fibre volume fraction (FVF).

### 3.5. Surface analysis

The surface of each sample was assessed for roughness and surface texture using an InfiniteFocusSL (Alicona Imaging GmbH, Austria) with 10 $\times$  optical magnification. A 5  $\times$  5 mm area in the centre of panel was measured using a vertical resolution of 100 nm and a lateral resolution of 1  $\mu\text{m}$ .

For surface roughness calculations, a filter value of  $\lambda_c = 0.8$  mm was chosen. Practically this value determines the intersection

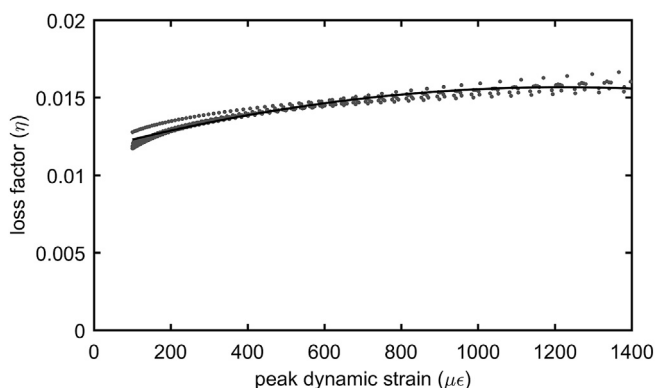


Fig. 4. Damping ratio for different peak strain levels for 4 bar NFRP material.

between roughness and waviness components. Form removal was completed for all scans to ensure that the roughness profiles were centred about a zero point to account for any surface tilting. The image was analysed using three, 4 mm long, 10  $\mu\text{m}$  wide profiles drawn across the measured area in both 0° and 90° fibre directions for all specimens in order to meet ISO 4288 requirements.

The images collected for the surface roughness measurements were also used for surface texture processing. As before, a  $\lambda_c$  filter value of 0.8 mm was applied to the image before textural parameters were collected from the software according to ISO 25178.

## 4. Results and discussion

All panels were manufactured successfully except for the 4 bar carbon panel. The pressure proved inadequate to wet the fabric fully and so this has been excluded from the results. All results are presented in Table 2 below. In the case of NFRP and HFRP samples an increase in pressure from 4 to 8 bar gave a small increase in average panel thickness of 0.14–0.15 mm most likely as a result of mould deflection due to pressure.

### 4.1. Results of tensile testing

Results for the tensile strength of all samples are shown in Fig. 5. Mean values are plotted with error bars set at one standard deviation. The NFRP and HFRP panels produced at 8 bar had a lower tensile strength than those produced at 4 bar. This was most noticeable for the NFRP samples where tensile strength dropped by approximately 38% versus 6% for HFRP. Previous research has demonstrated variation in mechanical properties due to resin injection pressure. It was observed that doubling the injection pressure into a mould containing E-glass fibre produced parts with an 11% reduction in tensile strength [32]. This was explained by an increase in void content at the higher pressure. An investigation of glass epoxy composites via RTM using 3–5 bar found higher pressure had little effect on interlaminar shear strength but it reduced flexural strength and increased storage modulus [33]. Another study investigated void formation and tensile strength of glass vinylester composites made via RTM and found that impregnation velocity was critical to optimise these properties [34]. In the present study higher injection pressure has had a marked effect on the tensile strength of NFRP which cannot be explained by increased void content or decreased FVF. It is possible that the higher pressure is introducing damage into the natural fibres within the composite.

The inclusion of carbon plies for the HFRP panel has given a useful increase in tensile strength but more significantly the tensile modulus has almost doubled. In addition, the tensile modulus for both NFRP and HFRP have shown a small increase with injection pressure. The CFRP panel demonstrated significantly higher tensile strength and modulus than NFRP and HFRP panels and had a tensile strength comparable with previous work with 2  $\times$  2 twill T300 epoxy composite at a similar FVF (584 versus 535.2 MPa) demonstrating valid results [5]. It is of note that while the CFRP has a specific strength of 361.6 versus 115 for a 6061 T6 aluminium both the HFRP and NFRP panels fall below this. As such careful consideration should be used if they are being applied purely for weight saving applications.

### 4.2. Results for vibration testing

The vibration testing results are summarised in Table 2. Fig. 6 highlights the average loss factor for all materials, it can be seen that in each case, damping gradually increases with strain amplitude although this is slight. The natural fibre specimens have

**Table 2**  
Results for thickness, FVF, tensile strength and modulus, damping ratio, flexural modulus, density and surface roughness.

Material type	4 bar NFRP	8 bar NFRP	4 bar HFRP	8 bar HFRP	8 bar CFRP
Mean thickness (mm)	3.12	3.27	3.15	3.29	3.19
Calculated FVF	36.2%	34.6%	43.1%	41.2%	49.6%
Tensile strength (MPa)	72.7	45.5	98.2	92.4	535.2
Tensile modulus (GPa)	8.2	8.7	15.1	15.5	44.2
Loss factor, $\epsilon_{\max} = 10^{-4}$	0.0123	0.0112	0.0048	0.0038	0.0024
Loss factor, $\epsilon_{\max} = 10^{-3}$	0.0155	0.0145	0.0072	0.0087	0.0050
Flexural modulus (GPa)	8.46	12.4	32.3	33.7	50.5
Fibre volume fraction (%)	45.8%	50.9%	CF 69.2% (10.0%) NF 42.6% (36.4%)	CF 77.8% (10.8%) NF 45.6% (39.3%)	56.8%
(overall FVF of particular phase for HFRP)					
Density ( $\text{g}/\text{cm}^3$ )	1.22	1.22	1.27	1.27	1.48
Specific strength (tensile strength/density)	59.6	37.3	77.3	72.7	361.6
Surface quality, $S_a$ ( $\mu\text{m}$ )	2.89	1.89	3.02	1.82	1.10
Surface roughness, $R_a$ ( $\mu\text{m}$ )	2.15	1.51	1.80	1.42	0.94

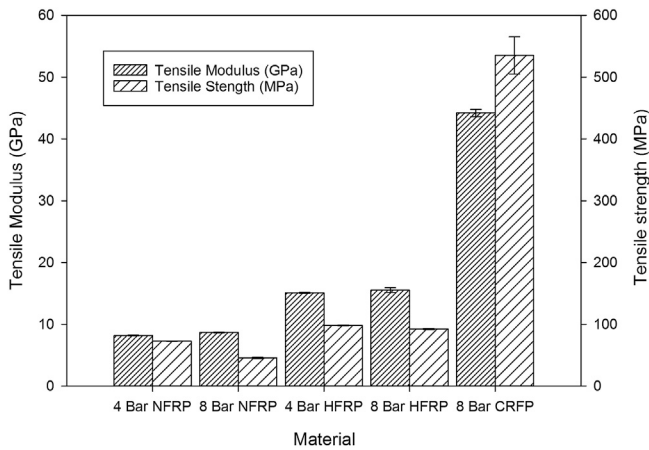


Fig. 5. Graph of tensile strength and modulus for each material.

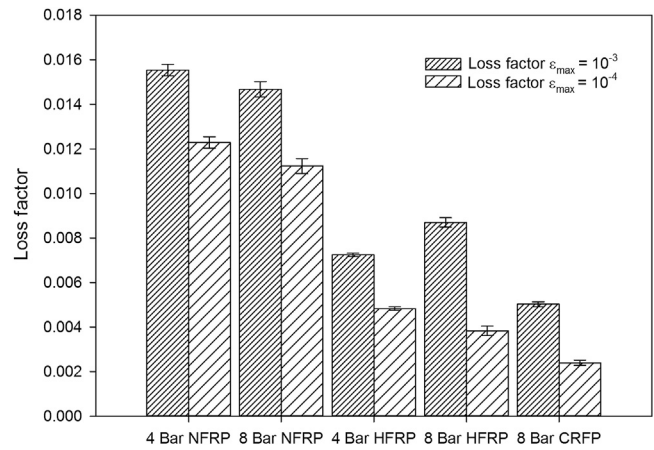


Fig. 7. Loss factor comparison at different strain levels.

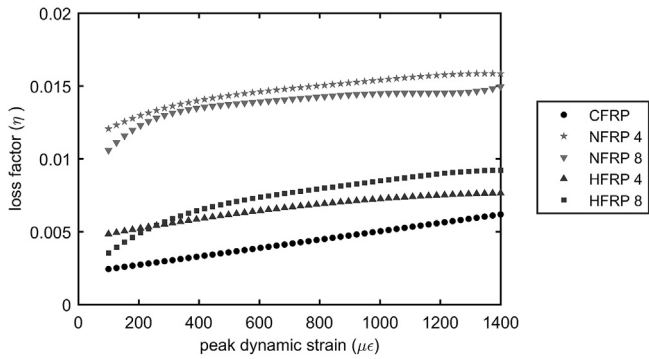


Fig. 6. Average loss factors for all material.

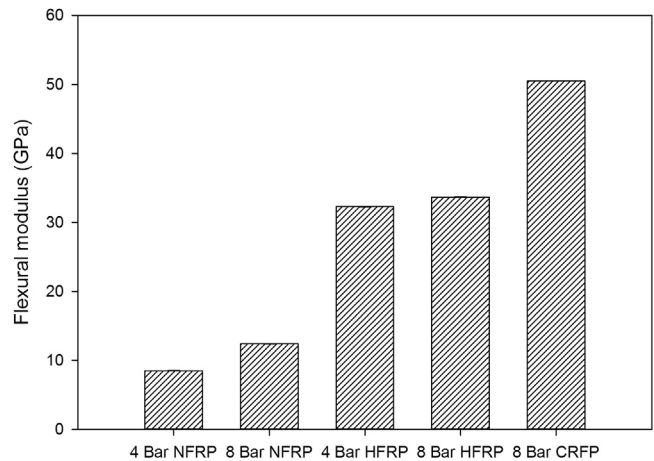


Fig. 8. Graph of flexural modulus for each sample.

considerably more damping than the carbon fibre ones while the results for the hybrid specimens lie between them. It is also noticeable that the NFRP and HFRP specimens produced at high pressure have lower damping at low strain levels than those produced at low pressure. This difference reduces as the strain level increases. Fig. 7 shows the loss factor at different strain levels and Fig. 8 the flexural modulus. The results demonstrate that flexural modulus increases somewhat with injection pressure for both NFRP and HFRP. More significantly the flexural modulus of HFRP is approximately three times that for the NFRP, a major improvement and closer to the value of the CFRP panel (33.7 versus 50.5 GPa).

In Fig. 7, the significant contribution that natural fibres make to

damping levels can be seen: compared with CFRP, the NFRP has more than four times the damping while the hybrid has twice as much. This is important for potential applications as an increase in damping results in a proportional decrease in resonant vibration amplitudes. It is also apparent that damping increases at higher strain levels. Some of this increase may be attributed to clamp friction and aerodynamic effects which are more significant at higher vibration amplitude (and hence higher dynamic strains). However, sensitivity of the strain dependence to material type

indicates the influence of other factors. For example, increasing pressure during manufacture consistently reduces damping at low strains but at higher strains, the trends in NFRP and HFRP differ.

Previous studies [16,18,19,21] that have reported damping levels for natural fibre and hybrid composites have provided results for tests where the peak strain was significantly less than  $400 \mu\epsilon$  and have not considered amplitude dependence. The mechanism causing sensitivity of the strain dependence to manufacturing pressure is therefore uncertain. One explanation may be the state of the interface between the fibre and matrix. At higher dynamic strains, some slip may occur which provides additional friction damping. However, as the overall stiffness does not change appreciably, this effect may be relatively minor. An alternative reason may be that the higher pressure cure alters the properties of the natural fibre itself such that it provides less damping at low strains. It is instructive to note that the strain dependence curve for carbon fibre, whose properties are relatively stable, is a different shape, being almost linear.

The vibration test results suggest that HFRPs could be a viable alternative to CFRPs in structural applications that require the composite to perform well in flexure but at lower cost than a pure carbon panel. The HFRP considered contained only 2 plies of carbon fibre as opposed to 14 plies in the CFRP making it significantly cheaper. The location of carbon fibre within the fibre pack has a small effect on tensile properties but considerable effect on flexural modulus.

#### 4.3. Results from optical microscopy

Images from optical microscopy are shown in Fig. 9, and results for fibre volume fraction analysis in Table 2. All samples were free of measurable voids. The six images used for analysis were selected at random although a thorough search of all samples using microscopy revealed no areas with voids. This is a reflection of the well-controlled RTM process which was scrupulously checked for vacuum leaks before each panel was manufactured.

FVF for NFRP varied from 45.8 to 50.9% which is reasonable given the heavy jute fabric and relatively coarse weave pattern. FVF for the HFRP panel was measured separately in the carbon and natural fibre regions. FVF in the natural fibre region was 42.6–45.6% and in the carbon region 69.2–77.8%. This may be because it was measured with a  $1200 \times 200$  pixel box in the carbon region generally dominated by fibre. The CFRP panel had an FVF of 56.8% which is high for a woven composite via RTM. The results demonstrate that a higher injection pressure leads to a small increase in FVF for the natural fibre sections of both the NFRP (45.8–50.9%) and HFRP (42.6–45.6%). This may be counterintuitive given the small increase in thickness at high pressure although previous work has demonstrated that pressure has a significant effect on FVF [35]. It is likely that the compression of the fibre stack via the mould and convergent design of the mould driving the fibre stack towards the centre are responsible for a measured FVF which is higher than the calculated value for all samples.

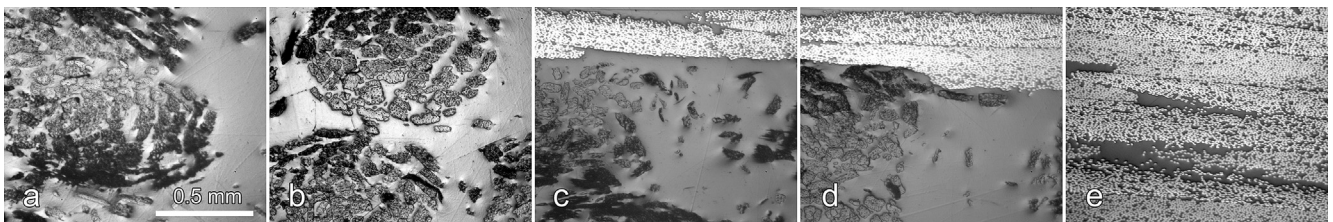


Fig. 9. Typical fibre volume fraction optical microscopy images for a) 4 bar NFRP, b) 8 bar NFRP, c) 4 bar HFRP, d) 8 bar HFRP, e) 8 bar CFRP.

#### 4.4. Results from surface analysis

After post cure the samples had visibly different surfaces, in particular the 4 bar samples demonstrated greater roughness. The results for surface quality ( $S_a$  – average height of selected area) and surface roughness ( $R_a$  – average roughness of profile) are graphed in Fig. 10. The 8 bar CFRP sample had the best surface quality and reflected the ground surface of the steel tool. For both the NFRP and HFRP there was a significant improvement in surface quality and roughness with an increase in pressure. It was evident that the resin rich regions of the layup had not shrunk away from the surface and in both cases the 8 bar samples got close to the 8 bar CFRP sample.

#### 5. Conclusions

Tensile strength reduced with increasing injection pressure for NFRP (72.7 MPa at 4 bar, 45.5 MPa at 8 bar) and HFRP (98.4 MPa at 4 bar, 92.4 MPa at 8 bar). This could not be explained by measured FVF which actually increased with pressure or voidage which remained at 0%. It is most likely as result of pressure induced damage to the jute fibres. The HFRP samples demonstrated a useful increase in tensile strength over NFRP at both pressures although strength was well short of CFRP (535.2 MPa). The tensile modulus for HFRP (15.1 GPa) was almost double that for NFRP (8.2 GPa) and one third of CFRP (44.2 GPa).

There was a significant increase in damping for NFRP and HFRP versus CFRP. Higher pressures appear to reduce the damping ratio but also change the strain dependence. This may be due to alterations in the fibre-matrix bond. The loss factor at small strains ( $10^{-4}$ ) reduced slightly with increasing pressure for NFRP (0.0123 at 4 bar, 0.0112 at 8 bar) and HFRP (0.0048 at 4 bar, 0.0038 at 8 bar) but all values were greater than CFRP (0.0024). At high strains

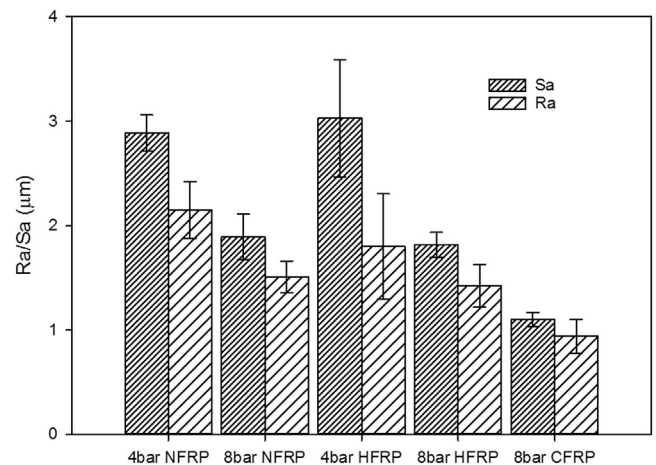


Fig. 10. Surface quality ( $S_a$ ) and roughness ( $R_a$ ) for all samples.

( $10^{-3}$ ) the loss factor decreases for NFRP (0.0155–0.0145) and increases for the HFRP (0.0072–0.0087) with increasing pressure.

The flexural modulus of the HFRP (32.3 GPa at 4 bar and 33.7 GPa at 8 bar) was significantly greater than NFRP (8.5 GPa at 4 bar and 12.4 GPa at 8 bar) and approaching CFRP (50.5 GPa). In flexure, the increase in damping from using HFRP is proportionally greater than the reduction in modulus so resonant vibrations would be lower for the same applied forcing.

NFRP had a low density of 1.22 g/cm<sup>3</sup> compared with HFRP (1.27 g/cm<sup>3</sup>) and CFRP (1.48 g/cm<sup>3</sup>) which did not change with pressure. However, pressure had a marked effect on surface roughness and quality. For NFRP ( $R_a = 2.15 \mu\text{m}$  at 4 bar,  $1.51 \mu\text{m}$  at 8 bar) and HFRP ( $R_a = 1.80 \mu\text{m}$  at 4 bar,  $1.42 \mu\text{m}$  at 8 bar) an increase in pressure improved the surface properties and prevented read through of the weave pattern. Neither the NFRP ( $R_a = 1.51 \mu\text{m}$ ) or HFRP ( $R_a = 1.42 \mu\text{m}$ ) samples were able to match the CFRP ( $R_a = 0.94 \mu\text{m}$ ). Hybridisation of low cost, sustainable jute with carbon fibre offers a more sustainable and economic alternative to CFRPs with excellent damping properties.

### Acknowledgements

The authors would like to acknowledge Innovate UK (101798) for contributing to this work.

### References

- [1] Howarth J, Mareddy SS, Mativenga PT. Energy intensity and environmental analysis of mechanical recycling of carbon fibre composite. *J Clean Prod* 2014;81:46–50.
- [2] Meredith J, Coles SR, Powe R, Collings E, Cozien-Cazuc S, Weager B, et al. On the static and dynamic properties of flax and Cordenka epoxy composites. *Compos Sci Technol* 2013;80(0):31–8.
- [3] Saheb DN, Jog J. Natural fiber polymer composites: a review. *Adv Polym Technol* 1999;18(4):351–63.
- [4] Pimenta S, Pinho ST. Recycling carbon fibre reinforced polymers for structural applications: technology review and market outlook. *Waste Manag* 2011;31(2):378–92.
- [5] Meredith J, Cozien-Cazuc S, Collings E, Carter S, Alsop S, Lever J, et al. Recycled carbon fibre for high performance energy absorption. *Compos Sci Technol* 2012;72(6):688–95.
- [6] Li X, Bai R, McKechnie J. Environmental and financial performance of mechanical recycling of carbon fibre reinforced polymers and comparison with conventional disposal routes. *J Clean Prod* 2016;127:451–60.
- [7] Turner TA, Pickering SJ, Warrior NA. Development of recycled carbon fibre moulding compounds – preparation of waste composites. *Compos Part B Eng* 2011;42(3):517–25.
- [8] Faruk O, A.K. Bledzki, H.-P. Fink, M. Sain. Biocomposites reinforced with natural fibers: 2000–2010. *Progress in Polymer Science*. 37(11): p. 1552–1596.
- [9] Jawaid M, Abdul Khalil HPS. Cellulosic/synthetic fibre reinforced polymer hybrid composites: a review. *Carbohydr Polym* 2011;86(1):1–18.
- [10] Dhakal HN, Zhang ZY, Guthrie R, MacMullen J, Bennett N. Development of flax/carbon fibre hybrid composites for enhanced properties. *Carbohydr Polym* 2013;96(1):1–8.
- [11] Patel VA, Vasoya PJ, Bhuvu BD, Parsania PH. Preparation and physicochemical study of hybrid glass-jute (treated and untreated) bisphenol-C-based mixed epoxy phenolic resin composites. *Polymer-Plastics Technol Eng* 2008;47(8): 842–6.
- [12] Davoodi MM, Sapuan SM, Ahmad D, Ali A, Khalina A, Jonoobi M. Mechanical properties of hybrid kenaf/glass reinforced epoxy composite for passenger car bumper beam. *Mater Des* 2010;31(10):4927–32.
- [13] Ashok Kumar M, Ramachandra Reddy G, Siva Bharathi Y, Venkata Naidu S, Naga Prasad Naidu V. Frictional coefficient, hardness, impact strength, and chemical Resistance of reinforced sisal-glass fiber epoxy hybrid composites. *J Compos Mater* 2010;44(36):3195–202.
- [14] Kushwaha PK, Kumar R. The studies on performance of epoxy and polyester-based composites reinforced with bamboo and glass fibers. *J Reinf Plastics Compos* 2009;29(13):1952–62.
- [15] Flynn J, Amiri A, Ulven C. Hybridized carbon and flax fiber composites for tailored performance. *Mater Des* 2016;102:21–9.
- [16] Le Guen MJ, Newman RH, Fernyhough A, Emms GW, Staiger MP. The damping–modulus relationship in flax–carbon fibre hybrid composites. *Compos Part B Eng* 2016;89:27–33.
- [17] Meredith J, Ebsworth R, Coles SR, Wood BM, Kirwan K. Natural fibre composite energy absorption structures. *Compos Sci Technol* 2012;72(2):211–7.
- [18] Assarar M, Zouari W, Sabhi H, Ayad R, Berthelot J-M. Evaluation of the damping of hybrid carbon–flax reinforced composites. *Compos Struct* 2015;132:148–54.
- [19] Le Guen M-J, Newman RH, Fernyhough A, Staiger MP. Tailoring the vibration damping behaviour of flax fibre-reinforced epoxy composite laminates via polyol additions. *Compos Part A Appl Sci Manuf* 2014;67:37–43.
- [20] El-Sabbagh A, Steuernagel L, Ziegmann G. Characterisation of flax polypropylene composites using ultrasonic longitudinal sound wave technique. *Compos Part B Eng* 2013;45(1):1164–72.
- [21] Duc F, Bourban P-E, Manson J-AE. Dynamic mechanical properties of epoxy/flax fibre composites. *J Reinf Plastics Compos* 2014;33(17):1625–33.
- [22] Padal, K., K. Ramji, and V. Prasad, Damping behavior of jute nano fibre reinforced composites.
- [23] Ornaghi HL, Bolner AS, Fiorio R, Zattera AJ, Amico SC. Mechanical and dynamic mechanical analysis of hybrid composites molded by resin transfer molding. *J Appl Polym Sci* 2010;118(2):887–96.
- [24] Haider M, Hubert P, Lessard L. An experimental investigation of class A surface finish of composites made by the resin transfer molding process. *Compos Sci Technol* 2007;67(15–16):3176–86.
- [25] Laurenzi S, Casini A, Pocci D. Design and fabrication of a helicopter unitized structure using resin transfer moulding. *Compos Part A Appl Sci Manuf* 2014;67:221–32.
- [26] Olivero KA. Effects of process parameters and mold design on resin transfer molded composites. University of Oklahoma; 2004.
- [27] Roychowdhury S, Gillespie Jr J, Advani S. Void formation and growth in thermoplastic processing. In: Computer aided design in composite material technology III. Springer; 1992. p. 89–107.
- [28] Prabhakaran RD, Babu B, Agrawal V. Quality evaluation of resin transfer molded products. *J Reinf Plastics Compos* 2008;27(6):559–81.
- [29] Pickering KL, Efendy MGA, Le TM. A review of recent developments in natural fibre composites and their mechanical performance. *Compos Part A Appl Sci Manuf* 2016;83:98–112.
- [30] Longana ML, Ong N, Yu H, Potter KD. Multiple closed loop recycling of carbon fibre composites with the HiPerDiF (High Performance Discontinuous Fibre) method. *Compos Struct* 2016;153:271–7.
- [31] Wambua P, Ivens J, Verpoest I. Natural fibres: can they replace glass in fibre reinforced plastics? *Compos Sci Technol* 2003;63(9):1259–64.
- [32] Patel N, Rohatgi V, Lee LJ. Influence of processing and material variables on resin-fiber interface in liquid composite molding. *Polym Compos* 1993;14(2): 161–72.
- [33] Lee C-L, Wei K-H. Resin transfer molding (RTM) process of a high performance epoxy resin. II: effects of process variables on the physical, static and dynamic mechanical behavior. *Polym Eng Sci* 2000;40(4):935–43.
- [34] Leclerc JS, Ruiz E. Porosity reduction using optimized flow velocity in Resin Transfer Molding. *Compos Part A Appl Sci Manuf* 2008;39(12):1859–68.
- [35] Pearce N, Summerscales J. The compressibility of a reinforcement fabric. *Compos Manuf* 1995;6(1):15–21.